ELSEVIER

Journal of Organometallic Chemistry 540 (1997) 147–154

Journal of Organometallic Chemistry

# Mixed-metal cluster chemistry VI [1]: phosphine substitution at $CpMoIr_3(\mu\text{-}CO)_3(CO)_8$; X-ray crystal structure of $CpMoIr_3(\mu\text{-}CO)_3(CO)_7(PPh_3)$

Nigel T. Lucas [a], Ian R. Whittall [a], Mark G. Humphrey [a,*], David C.R. Hockless [b], M.P. Seneka Perera [c], Michael L. Williams [c]

[a] *Department of Chemistry, Australian National University, Canberra, A.C.T. 0200, Australia*
[b] *Research School of Chemistry, Australian National University, Canberra, A.C.T. 0200, Australia*
[c] *Faculty of Science and Technology, Griffith University, Nathan, Qld. 4111, Australia*

Received 18 December 1996; revised 23 January 1997

**Abstract**

Reactions of $CpMoIr_3(\mu\text{-}CO)_3(CO)_8$ (**1**) with stoichiometric amounts of phosphines afford the substitution products $CpMoIr_3(\mu\text{-}CO)_3(CO)_{8-x}(L)_x$ (L = $PPh_3$, $x$ = 1 (**2**), 2 (**3**); L = $PMe_3$, $x$ = 1 (**4**), 2 (**5**), 3 (**6**)) in fair to good yields (23–54%); the yields of both **3** and **6** are increased on reacting **1** with excess phosphine. Products **2–5** are fluxional in solution, with the interconverting isomers resolvable at low temperatures. A structural study of one isomer of **2** reveals that the three edges of an $MoIr_2$ face of the tetrahedral core are spanned by bridging carbonyls, and that the iridium-bound triphenylphosphine ligates radially and the molybdenum-bound cyclopentadienyl coordinates axially with respect to this $MoIr_2$ face. Information from this crystal structure, $^{31}P$ NMR data (both solution and solid-state), and results with analogous tungsten–triiridium and tetrairidium clusters have been employed to suggest coordination geometries for the isomeric derivatives. © 1997 Elsevier Science S.A.

*Keywords:* Molybdenum; Iridium; Carbonyl; Cyclopentadienyl; Cluster; Phosphine; Crystal structure

## 1. Introduction

Although a great deal of interest has been shown in the chemistry of mixed-metal clusters recently, most reports have dealt with clusters containing metals from the same group or adjacent groups; clusters containing disparate metals are comparatively little investigated. We have been interested in probing the effect on reactivity and selectivity of sequentially replacing $Ir(CO)_3$ units in the tetrahedral cluster $Ir_4(CO)_{12}$ by isolobal $CpW(CO)_2$ groups and have recently reported enhanced reactivity toward phosphine substitution of $CpWIr_3(CO)_{11}$ compared to $Ir_4(CO)_{12}$ [2,3], unusual phosphine P–C cleavage in the mixed-metal system not observed with the homometallic cluster [4], and differing base-assisted cluster condensation for $Cp_2W_2Ir_2(CO)_{10}$ vs. $Ir_4(CO)_{12}$ [5]. Phosphine substitution at $CpWIr_3(CO)_{11}$ in particular is characterized by mixtures of interconverting isomers due to differing ligand coordination sites and plane of bridging carbonyls (both $WIr_2$ and $Ir_3$) at the tetrahedral cluster core. We postulated that replacement of tungsten by its lighter homologue molybdenum may simplify the isomer mixtures by localizing the $(\mu\text{-}CO)_3$ plane at $MoIr_2$ (as 4d metals favour bridging carbonyls compared with 5d metals), and that the lighter metal may enhance reactivity of the mixed-metal cluster. We report herein the results of reacting $CpMoIr_3(\mu\text{-}CO)_3(CO)_8$ with 1, 2, 3 equiv. or excess of $PPh_3$ and $PMe_3$, and the characterization by X-ray crystallography of one isomer of $CpMoIr_3(\mu\text{-}CO)_3(CO)_7(PPh_3)$.

* Corresponding author. Tel.: (+61) 6 249 2927; fax: (+61) 6 249 0760; e-mail: mark.humphrey@anu.edu.au.

[1] For part V, see Ref. [1].


*PII* S0022-328X(97)00111-3

## 2. Results and discussion

### 2.1. Syntheses and characterization of $CpMoIr_3(\mu\text{-}CO)_3(CO)_{8-n}(L)_n$ ($L = PPh_3$, $n = 1$ (2), 2 (3); $L = PMe_3$, $n = 1$ (4), 2 (5), 3 (6))

The reactions of $CpMoIr_3(\mu\text{-}CO)_3(CO)_8$ (**1**) with $n$ equiv. of $PPh_3$ ($n = 1$, 2, 3 or excess) proceed in dichloromethane at room temperature (Scheme 1). Reaction with 1 equiv. affords the expected mono-substituted cluster in fair yield, but with some unsubstituted and bis-substituted product also. Similarly, reaction with 2 equiv. affords the bis-substituted cluster as the major product, but with some mono-substituted cluster. Reactions with 3 equiv. or excess $PPh_3$ afford the bis-substituted cluster as the sole product, with no evidence for tris-substitution. The mono-substituted cluster $CpMoIr_3(\mu\text{-}CO)_3(CO)_7(PPh_3)$ (**2**) and bis-substituted cluster $CpMoIr_3(\mu\text{-}CO)_3(CO)_6(PPh_3)_2$ (**3**) were characterized by a combination of IR, $^1H$ and $^{31}P$ NMR spectroscopy, MS, and satisfactory microanalyses. The IR spectra contain $\nu$(CO) bands in the bridging as well as terminal carbonyl ligand regions; the number of bands in the spectra of both complexes is indicative of the presence of isomers. The $^1H$ NMR spectra contain resonances in the phenyl and cyclopentadienyl regions in the predicted ratios. The mass spectra contain molecular ions and fragment ions corresponding to sequential loss of all carbonyl ligands. The spectrum of the bis-substituted cluster differs in that it also shows fragmentation and loss of phosphine ligands, which become competitive with loss of carbonyl for $[M - 6CO]^+$. The identity of one isomer of (**2**) was confirmed by a structural study, the first crystallographically characterized derivative from the molybdenum–iridium system.

The reactions of $CpMoIr_3(\mu\text{-}CO)_3(CO)_8$ (**1**) with $n$ equiv. of $PMe_3$ ($n = 1$, 2, 3 or excess) proceed in tetrahydrofuran at room temperature (Scheme 1). Reactions with 1, 2 or 3 equiv. afford the expected mono-, bis- or tris-substituted cluster as the major product, but with some contamination similar to that found with $PPh_3$. Clusters $CpMoIr_3(\mu\text{-}CO)_3(CO)_7(PMe_3)$ (**4**), $CpMoIr_3(\mu\text{-}CO)_3(CO)_6(PMe_3)_2$ (**5**) and $CpMoIr_3(\mu\text{-}CO)_3(CO)_5(PMe_3)_3$ (**6**) were characterized by IR, $^1H$ NMR and $^{31}P$ NMR spectroscopy, MS and (for **4** and **5**) satisfactory microanalyses; complex **6** could not be crystallized, and decomposed over days. Edge-bridging carbonyl ligands are found in the IR spectra of all three complexes; as with the $PPh_3$-substituted clusters, the number of bands in the $\nu$(CO) region are consistent with the presence of isomers. The $^1H$ NMR spectra contain resonances in the cyclopentadienyl and methyl regions in the predicted ratios. The mass spectra contain molecular ions at the expected values; fragmentation by loss of phosphine or methyl becomes increasingly competitive with loss of carbonyl on increasing phosphine substitution.

### 2.2. X-ray structural study of $CpMoIr_3(\mu\text{-}CO)_3(CO)_7(PPh_3)$ (2a)

The molecular structure of **2a**, as determined by the single crystal X-ray study, is consistent with the formulation above, defines the substitution site of the phosphine, and facilitates interpretation of the $^{31}P$ NMR spectra. Fractional atomic coordinates are given in Table 1 and selected bond lengths and angles listed in Table 2. Fig. 1 contains an ORTEP plot of **2a** showing the molecular structure and atomic labelling scheme.

Complex **2a** has the $MoIr_3$ pseudotetrahedral framework of the precursor cluster **1** and possesses an $\eta^5$-cyclopentadienyl group, three bridging carbonyls arranged about an $MoIr_2$ plane, seven terminal carbonyl ligands and an iridium-ligated triphenylphosphine ligand. The $MoIr_3$ core distances (Ir–$Ir_{av}$ 2.70 Å; Mo–$Ir_{av}$ 2.87 Å) are similar to those of **1** (Ir–$Ir_{av}$ 2.70 Å; Mo–$Ir_{av}$ 2.86 Å), with the carbonyl-bridged metal–metal vectors shorter than the non-bridged cluster core bonds. Ir–CO(terminal) interactions for **2a** (1.84(1)–1.94(1) Å) and ∠Ir–C–O(terminal) (175(1)–179(1)°) are unexceptional. Carbonyls CO(12), CO(14) and CO(24) bridge somewhat asymmetrically, with CO(12) displaced to-

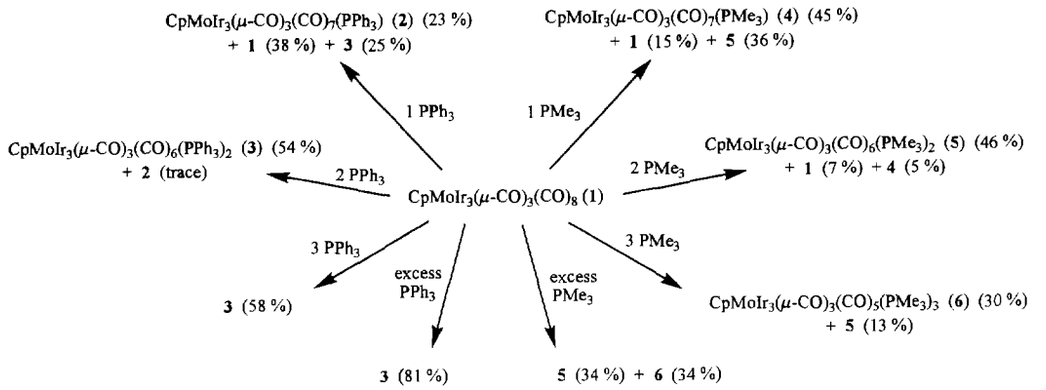


Scheme 1.

wards Ir(1), CO(14) towards Ir(1), and CO(24) displaced towards Mo(4); asymmetry of CO(12) and CO(14) may maximize backbonding to the bridging carbonyls from the electron rich phosphine-ligated Ir(1). The Ir–P distance (2.331(3) Å) and intraphosphine bond lengths and angles are not unusual. Formal electron counting reveals that **2a** has 60e$^-$, electron precise for a tetrahedral cluster. The disposition of ligands and asymmetry of bridging carbonyls in **2a** are similar to those found previously in $CpWIr_3(\mu\text{-}CO)_3(CO)_7(PPh_3)$ [3].

Table 1
Non-hydrogen atom coordinates and equivalent isotropic displacement parameters for $CpMoIr_3(\mu\text{-}CO)_3(CO)_7(PPh_3)$ (**2a**)

| Atom | x | y | z | $B_{eq}$ |
|---|---|---|---|---|
| Ir(1) | 0.19329(4) | 0.17879(3) | 0.40171(2) | 2.296(9) |
| Ir(2) | 0.37543(4) | 0.15683(3) | 0.50187(2) | 2.894(10) |
| Ir(3) | 0.37613(5) | 0.31212(3) | 0.44431(2) | 3.15(1) |
| Mo(4) | 0.14335(10) | 0.27277(6) | 0.49997(4) | 2.83(2) |
| P(1) | 0.1432(3) | 0.1814(2) | 0.3001(1) | 2.44(6) |
| O(11) | 0.0061(8) | 0.0254(6) | 0.4123(4) | 5.1(2) |
| O(12) | 0.4417(8) | 0.0584(6) | 0.3938(4) | 5.5(3) |
| O(14) | −0.0084(8) | 0.3359(5) | 0.3747(3) | 4.6(2) |
| O(21) | 0.6757(8) | 0.1417(8) | 0.5642(4) | 7.3(3) |
| O(22) | 0.2669(9) | −0.0089(6) | 0.5500(4) | 6.2(3) |
| O(24) | 0.3844(9) | 0.2717(6) | 0.6117(3) | 5.0(2) |
| O(31) | 0.6025(10) | 0.2468(8) | 0.3847(4) | 7.6(3) |
| O(32) | 0.568(1) | 0.4090(7) | 0.5449(4) | 7.5(3) |
| O(33) | 0.257(1) | 0.4646(6) | 0.3634(5) | 8.8(4) |
| O(41) | 0.199(1) | 0.4755(6) | 0.5089(5) | 6.9(3) |
| C(11) | 0.077(1) | 0.0841(7) | 0.4058(5) | 3.1(3) |
| C(12) | 0.373(1) | 0.1033(8) | 0.4161(5) | 3.5(3) |
| C(14) | 0.066(1) | 0.2891(7) | 0.4066(5) | 2.8(3) |
| C(21) | 0.566(1) | 0.1445(9) | 0.5410(5) | 4.7(3) |
| C(22) | 0.311(1) | 0.0531(8) | 0.5334(5) | 3.8(3) |
| C(24) | 0.323(1) | 0.2513(8) | 0.5641(5) | 4.1(3) |
| C(31) | 0.515(1) | 0.2726(10) | 0.4076(5) | 5.2(4) |
| C(32) | 0.494(1) | 0.3750(9) | 0.5066(6) | 4.8(4) |
| C(33) | 0.299(1) | 0.4081(9) | 0.3922(5) | 4.5(3) |
| C(41) | 0.188(1) | 0.3985(8) | 0.5029(5) | 4.2(3) |
| C(101) | −0.084(1) | 0.228(1) | 0.4907(6) | 4.9(4) |
| C(102) | −0.075(1) | 0.315(1) | 0.4087(7) | 5.5(4) |
| C(103) | 0.010(2) | 0.3195(10) | 0.5649(6) | 5.3(4) |
| C(104) | 0.047(1) | 0.231(1) | 0.5787(6) | 5.3(4) |
| C(105) | −0.011(1) | 0.1743(8) | 0.5324(7) | 4.7(4) |
| C(111) | −0.0441(9) | 0.1783(7) | 0.2659(4) | 2.6(2) |
| C(112) | −0.148(1) | 0.1716(7) | 0.2973(5) | 3.4(3) |
| C(113) | −0.286(1) | 0.1661(8) | 0.2704(6) | 4.3(3) |
| C(114) | −0.323(1) | 0.1675(9) | 0.2110(6) | 4.6(3) |
| C(115) | −0.221(1) | 0.1734(9) | 0.1778(5) | 5.1(3) |
| C(116) | −0.082(1) | 0.1790(9) | 0.2070(5) | 4.2(3) |
| C(121) | 0.205(1) | 0.2764(7) | 0.2663(4) | 2.7(3) |
| C(122) | 0.343(1) | 0.2800(8) | 0.2592(5) | 4.0(3) |
| C(123) | 0.392(1) | 0.352(1) | 0.2325(6) | 5.0(4) |
| C(124) | 0.306(2) | 0.4214(10) | 0.2155(6) | 5.7(4) |
| C(125) | 0.171(2) | 0.4208(9) | 0.2240(6) | 5.2(4) |
| C(126) | 0.122(1) | 0.3498(8) | 0.2493(5) | 3.9(3) |
| C(131) | 0.206(1) | 0.0858(7) | 0.2638(5) | 3.0(3) |
| C(132) | 0.240(1) | 0.0924(8) | 0.2095(5) | 4.6(3) |
| C(133) | 0.274(1) | 0.0163(10) | 0.1810(6) | 5.5(4) |
| C(134) | 0.271(1) | −0.0655(10) | 0.2063(7) | 5.6(4) |
| C(135) | 0.240(1) | −0.0718(8) | 0.2600(6) | 4.7(4) |
| C(136) | 0.207(1) | 0.0025(8) | 0.2893(5) | 3.4(3) |

Table 2
Selected bond lengths (Å) and angles (deg) for $CpMoIr_3(\mu\text{-}CO)_3(CO)_7(PPh_3)$ (**2a**)

| | | | |
|---|---|---|---|
| Ir(1)–Ir(2) | 2.6681(6) | Ir(1)–C(11) | 1.84(1) |
| Ir(1)–Ir(3) | 2.7439(7) | Ir(2)–C(21) | 1.92(1) |
| Ir(2)–Ir(3) | 2.7012(6) | Ir(2)–C(22) | 1.89(1) |
| Ir(1)–Mo(4) | 2.826(1) | Ir(3)–C(31) | 1.85(1) |
| Ir(2)–Mo(4) | 2.862(1) | Ir(3)–C(32) | 1.92(1) |
| Ir(3)–Mo(4) | 2.907(1) | Ir(3)–C(33) | 1.94(1) |
| Ir(1)–P(1) | 2.331(3) | Mo(4)–C(41) | 1.94(1) |
| Ir(1)–C(12) | 2.06(1) | Mo(4)–C(101) | 2.30(1) |
| Ir(1)–C(14) | 2.09(1) | Mo(4)–C(102) | 2.29(1) |
| Ir(2)–C(12) | 2.16(1) | Mo(4)–C(103) | 2.30(1) |
| Ir(2)–C(24) | 2.17(1) | Mo(4)–C(104) | 2.32(1) |
| Mo(4)–C(14) | 2.18(1) | Mo(4)–C(105) | 2.35(1) |
| Mo(4)–C(24) | 2.10(1) | | |
| | | | |
| Ir(2)–Ir(1)–Ir(3) | 59.86(2) | Ir(1)–Mo(4)–C(14) | 47.3(3) |
| Ir(2)–Ir(1)–Mo(4) | 62.71(2) | Mo(4)–Ir(1)–C(14) | 49.9(3) |
| Ir(3)–Ir(1)–Mo(4) | 62.89(2) | Ir(1)–C(12)–O(12) | 143.9(10) |
| Ir(1)–Ir(2)–Ir(3) | 61.46(2) | Ir(2)–C(12)–O(12) | 137.7(9) |
| Ir(1)–Ir(2)–Mo(4) | 61.35(2) | Ir(2)–C(24)–O(24) | 130.5(10) |
| Ir(3)–Ir(2)–Mo(4) | 62.92(2) | Mo(4)–C(24)–O(24) | 145(1) |
| Ir(1)–Ir(3)–Ir(2) | 58.67(4) | Mo(4)–C(14)–O(14) | 138.9(8) |
| Ir(1)–Ir(3)–Mo(4) | 59.94(2) | Ir(1)–C(14)–O(14) | 138.3(9) |
| Ir(2)–Ir(3)–Mo(4) | 61.25(2) | Ir(1)–C(11)–O(11) | 175(1) |
| Ir(1)–Mo(4)–Ir(2) | 55.94(2) | Ir(2)–C(21)–O(21) | 176(1) |
| Ir(1)–Mo(4)–Ir(3) | 57.17(2) | Ir(2)–C(22)–O(22) | 176(1) |
| Ir(2)–Mo(4)–Ir(3) | 55.84(2) | Ir(3)–C(31)–O(31) | 179(1) |
| Ir(2)–Ir(1)–C(12) | 52.4(3) | Ir(3)–C(32)–O(32) | 176(1) |
| Ir(1)–Ir(2)–C(12) | 49.3(3) | Ir(3)–C(33)–O(33) | 178(1) |
| Mo(4)–Ir(2)–C(24) | 46.8(3) | Mo(4)–C(41)–O(41) | 169(1) |
| Ir(2)–Mo(4)–C(24) | 49.0(3) | | |

### 2.3. Discussion

The IR spectra and in some cases the $^{31}P$ NMR spectra in solution at 230 K are indicative of the presence of isomers. Room temperature $^{31}P$ NMR spectra of **2**, **4** and **5** are consistent with coalescence of the low temperature signals, while spectra of **3** and **6** show substantial broadening. The $^{31}P$ NMR spectra are very similar to analogues from the tungsten–triiridium system [3] where isomers were proposed to arise from differing ligand (phosphine and cyclopentadienyl) substitution sites, or variations in the location of the plane of bridging carbonyls ($WIr_2$ vs. $Ir_3$). Substitution sites for the tungsten–triiridium derivatives were assigned utilizing information from (a) crystallographically verified isomers, (b) the substitution pattern in the tetrairidium system, and (c) chemical shifts in the $^{31}P$ NMR spectra (for which the positional sequence $\delta$ (bridging) > $\delta$ (radial) > $\delta$ (axial) ≈ $\delta$ (apical) was found with tetrairidium clusters). Results from studies in the molybdenum–triiridium system are summarized in Table 3,

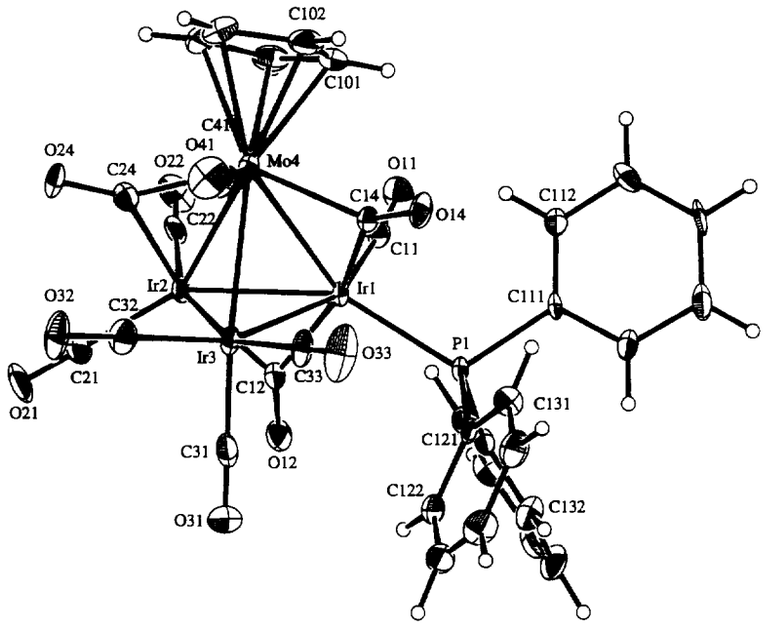


Fig. 1. Molecular structure and atomic labelling scheme for $CpMoIr_3(\mu\text{-}CO)_3(CO)_7(PPh_3)$ (**2a**). Thermal envelopes of 20% probability are shown for the non-hydrogen atoms; hydrogen atoms have arbitrary radii of 0.1 Å.

together with data from the tungsten–triiridium analogues.

Suggested geometries for the isomers are indicated in Fig. 2. Chemical shifts for radial-, axial- or apical-ligated phosphine in the $^{31}P$ NMR spectra are remarkably similar for the tungsten–triiridium clusters and their molybdenum–triiridium analogues. Radial-ligated triphenylphosphine is detected at 25.1–31.8 ppm for bis- or tris-substituted clusters, whereas axial-coordinated triphenylphosphine is found at −5.1 to −7.7 ppm. The resonance at 4.7 ppm for M = W in the mono-substituted derivative, though anomalous, was assigned to a structurally characterized radially ligated ligand [3]. A similar signal at 10.4 ppm for M = Mo was also viewed with suspicion. We therefore obtained a solid-state $^{31}P$ NMR spectrum of crystals of **2a**; the spectrum reveals a resonance at 27.5 ppm, assigned to the crystallographically detected radially ligated phosphine. The solution resonance at 10.4 ppm for M = Mo (and, by implication, that at 4.7 ppm for M = W) are therefore due to rapidly exchanging environments for the phosphine, presumably radial and axial. The bis-substituted deriva-

Table 3
$^{31}P$ NMR data for $CpMIr_3(\mu\text{-}CO)_3(CO)_{8-n}(L)_n$ (M = Mo, W; L = $PPh_3$, $PMe_3$; $n$ = 1, 2 or 3) (230 K)

| Complex | | $^{31}P$ NMR chemical shifts (ppm) | | Suggested site for L substitution, with respect to $(\mu\text{-}CO)_3$ plane | Isomer ratio | |
|---|---|---|---|---|---|---|
| | M = Mo | M = Mo [a] | M = W [b] | | M = Mo | M = W |
| $n$ = 1, L = $PPh_3$ | **2a/2b** | 10.4 | 4.7 [a] | radial [d,e] and axial | | 4 |
| | **2c** | | −5.1 [a] | axial | | 5 |
| $n$ = 2, L = $PPh_3$ | **3a** | 25.6, −7.0 (1:1) | 25.1, −7.7 (1:1) [a] | radial, axial [e] | 1 | 1 |
| | **3b** | 27.1 | 27.3 [a] | diradial | 2 | 1 |
| $n$ = 3, L = $PPh_3$ | | | 31.8, −17.9 (2:1) [a] | diaxial, apical diradial, apical | | |
| $n$ = 1, L = $PMe_3$ | | −30.1 | −30.2 [c] | axial [e] | trace | 3 |
| | **4** | −26.2 | −26.1 [c] | radial | major | 2 |
| $n$ = 2, L = $PMe_3$ | **5a** | −23.8, −41.8 (1:1) | −22.7, −38.7 (1:1) [c] | radial, axial | 2 | 4 |
| | **5b** | −21.8 | −20.8 [c] | diradial | 3 | 5 |
| $n$ = 3, L = $PMe_3$ | **6** | −28.1, −46.7, −80.1 (1:1:1) | −27.1, −45.2, −83.4 (1:1:1) [c] | radial, axial, apical | | |

[a] $CDCl_3$.
[b] Ref. [3].
[c] Acetone-$d_6$.
[d] Crystallographically confirmed (M = Mo).
[e] Crystallographically confirmed (M = W).

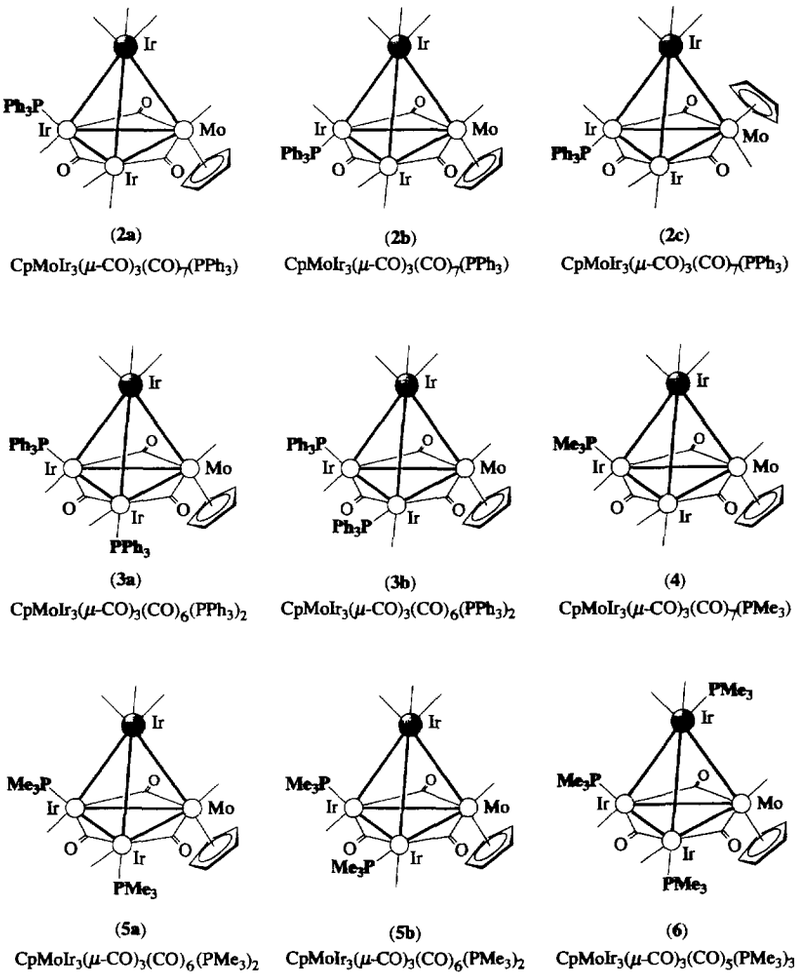


Fig. 2. Suggested configurations for **2–6**.

tive **3** occurs as radial, axial and diradial isomers as does the tungsten–iridium analogue, although the isomeric ratio differs (1:2 vs. 1:1). Similar signals are found for **4–6** as found previously for the tungsten–triiridium triphenylphosphine derivatives; for **4** and **5**, the mixture of isomers differs from that in the tungsten-containing complexes.

Phosphine substitution at cluster **1** thus proceeds with less control at room temperature than phosphine substitution at $CpWIr_3(CO)_{11}$; for the former, reaction with stoichiometric amounts affords mixtures of products whereas with the latter, stepwise reaction is observed. Steric considerations are more important for **1** than for $CpWIr_3(CO)_{11}$; the former does not afford a tris(triphenylphosphine) adduct, and the tris(trimethylphosphine) product is unstable, both unlike the latter. Mixtures of isomers are obtained from both systems; low temperature $^{31}P$ NMR suggests the same product type are observed for both **1** and $CpWIr_3(CO)_{11}$, but the isomeric ratio is different. The molybdenum–triiridium system favours radial vs. axial (for mono-substitution) and diradial vs. radial, axial (for bis-substitution), unlike the tungsten–triiridium cluster. It is well-established that the least sterically hindered sites at tetrahedral clusters are the radial sites, with ligands occupying axial sites on electronic grounds [6]. The more sterically encumbered molybdenum–triiridium cluster **1** favours phosphine ligation at radial sites. In contrast, $CpWIr_3(CO)_{11}$ prefers phosphine coordination at the electronically favourable axial sites. Thus, although similarities in chemistry between the two systems are apparent, cluster **1** appears to have enhanced reactivity toward phosphine substitution, with steric restrictions directing site selection in the isomeric possibilities. Further studies with mixed-metal clusters are currently under way.

## 3. Experimental details

### 3.1. General conditions

Reactions were performed under an atmosphere of argon (high-purity, CIG) although no special precau-

tions were taken to exclude air during work-up. The reaction solvents were dried by standard methods: $CH_2Cl_2$ over $CaH_2$ and THF over sodium–benzophenone, both under a nitrogen atmosphere. Petroleum spirit refers to a petroleum fraction of boiling range 60–80 °C. The products were purified by thin-layer chromatography on $20 \times 20\,cm^2$ glass plates coated with Merck $GF_{254}$ silica gel (0.5 mm). Literature procedures were used to synthesize $CpMoIr_3(\mu\text{-}CO)_3(CO)_8$ (**1**) [7]. Commercial reagents $PPh_3$ (Aldrich) and $PMe_3$ (1.0 M solution in THF) (Aldrich) were used as-received.

### 3.2. Instruments

IR spectra were recorded on a Perkin–Elmer System 2000 FT-IR with $CaF_2$ optics. $^1H$ and room temperature $^{31}P$ NMR solution spectra were recorded in $CDCl_3$ using a Varian Gemini-300 ($^1H$ at 300 MHz, $^{31}P$ at 121 MHz) and are referenced to residual $CHCl_3$ (7.24 ppm) and external 85% $H_3PO_4$ (0.00 ppm) respectively. Variable-temperature (230 K) $^{31}P$ NMR spectra were recorded in $CDCl_3$ using a Varian VXR300S spectrometer (121 MHz) and are referenced to external $H_3PO_4$ (0.00 ppm). The solid state $^{31}P$ NMR spectrum of **2a** was obtained using a Varian Unity-400 spectrometer at 161.929 MHz. The compound was packed in a Kel-F insert and placed in a silicon nitride rotor and spun at 3 kHz at the magic angle. The $^{31}P$ NMR spectrum was obtained at 298 K with proton power decoupling and cross-polarization. A contact time of 2.0 ms and a recycle time of 30 s were used. A resonance with a chemical shift of 27.5 ppm was observed, referenced to 85% $H_3PO_4$ through solid $PPh_3$ (−10.0 ppm). Mass spectra were recorded using a VG ZAB 2SEQ instrument (30 kV $Cs^+$ ions, current 1 mA, accelerating potential 8 kV, 3-nitrobenzyl alcohol matrix) at the Research School of Chemistry, Australian National University; peaks are reported as $m/z$ (assignment, relative intensity). Microanalyses were carried out by the Microanalysis Service Unit in the Research School of Chemistry, Australian National University.

### 3.3. Reaction of $CpMoIr_3(\mu\text{-}CO)_3(CO)_8$ with 1 equiv. of $PPh_3$

An orange solution of $CpMoIr_3(\mu\text{-}CO)_3(CO)_8$ (35.3 mg, 0.0338 mmol) and $PPh_3$ (8.8 mg, 0.034 mmol) in $CH_2Cl_2$ (25 ml) was stirred at room temperature for 24 h. The dark orange solution obtained was evaporated to dryness on a rotary evaporator, then the residue dissolved in $CH_2Cl_2$ (ca. 3 ml) and applied to preparative chromatographic plates. Elution with dichloromethane–petroleum spirit (3/2) gave three bands. The contents of the first and major band, $R_f$ = 0.78, were identified by solution IR as unreacted $CpMoIr_3(\mu\text{-}CO)_3(CO)_8$ (**1**) (13.6 mg, 0.0130 mmol (38%)). The second band, $R_f = 0.68$, was crystallized from $CH_2Cl_2$–MeOH to afford orange crystals of $CpMoIr_3(\mu\text{-}CO)_3(CO)_7(PPh_3)$ (**2**) (10.1 mg, 0.0079 mmol (23%)). The third band, $R_f = 0.49$, was crystallized from $CH_2Cl_2$–MeOH to afford orange crystals of $CpMoIr_3(\mu\text{-}CO)_3(CO)_6(PPh_3)_2$ (**3**) (12.8 mg, 0.0085 mmol (25%)).

### 3.4. Reaction of $CpMoIr_3(\mu\text{-}CO)_3(CO)_8$ with 2 equiv. of $PPh_3$

Following the method in Section 3.3, $CpMoIr_3(\mu\text{-}CO)_3(CO)_8$ (20.9 mg, 0.0200 mmol) was reacted with $PPh_3$ (10.5 mg, 0.0401 mmol) in $CH_2Cl_2$ (15 ml) at room temperature for 24 h. Purification by preparative chromatography with dichloromethane–petroleum spirit (3/2) eluent gave two bands. The first band, $R_f = 0.80$, in trace amounts, was identified by solution IR as $CpMoIr_3(\mu\text{-}CO)_3(CO)_7(PPh_3)$ (**2**). The major band, $R_f = 0.50$, was identified by IR and $^1H$ NMR as $CpMoIr_3(\mu\text{-}CO)_3(CO)_6(PPh_3)_2$ (**3**) (16.2 mg, 0.0107 mmol (54%)).

### 3.5. Reaction of $CpMoIr_3(\mu\text{-}CO)_3(CO)_8$ with 3 equiv. of $PPh_3$

Following the method in Section 3.3, $CpMoIr_3(\mu\text{-}CO)_3(CO)_8$ (24.7 mg, 0.0236 mmol) was reacted with $PPh_3$ (18.7 mg, 0.0713 mmol) in $CH_2Cl_2$ (15 ml) at room temperature for 24 h. Purification by preparative chromatography with dichloromethane–petroleum spirit (3/2) eluent gave one band, $R_f = 0.49$, identified by IR and $^1H$ NMR as $CpMoIr_3(\mu\text{-}CO)_3(CO)_6(PPh_3)_2$ (**3**) (20.7 mg, 0.0137 mmol (58%)).

### 3.6. Reaction of $CpMoIr_3(\mu\text{-}CO)_3(CO)_8$ with excess $PPh_3$

Following the method in Section 3.3, $CpMoIr_3(\mu\text{-}CO)_3(CO)_8$ (40.4 mg, 0.0386 mmol) was reacted with $PPh_3$ (64.8 mg, 0.247 mmol) in $CH_2Cl_2$ (25 ml) at room temperature for 24 h. Purification by preparative chromatography with dichloromethane–petroleum spirit (3/2) eluent gave one band, $R_f = 0.48$, identified by IR and $^1H$ NMR as $CpMoIr_3(\mu\text{-}CO)_3(CO)_6(PPh_3)_2$ (**3**) (47.4 mg, 0.0313 mmol (81%)).

### 3.7. Analytical data for 2 and 3

**2**. Anal. Found: C, 31.08; H, 1.07%. $C_{33}H_{20}Ir_3MoO_{10}P$. Calc.: C, 30.96; H, 1.57%. IR (c-$C_6H_{12}$): $\nu$(CO) 2077s, 2064m, 2042vs, 2025vs, 2012vs, 1995vs, 1963m, 1930m, 1851w, 1823w, 1809w, 1733m $cm^{-1}$. $^1H$ NMR ($CDCl_3$): $\delta$ 7.43–7.33 (m, 15H, Ph), 4.86 (s, 5H, $C_5H_5$) ppm. $^{31}P$ NMR ($CDCl_3$, 230 K): 10.4 (s, 1P) ppm. MS: 1282 ([M]$^+$, 34), 1254 ([M −

$CO]^+$, 12), 1226 ($[M - 2CO]^+$, 51), 1198 ($[M - 3CO]^+$, 33), 1170 ($[M - 4CO]^+$, 100), 1142 ($[M - 5CO]^+$, 50), 1114 ($[M - 6CO]^+$, 38), 1086 ($[M - 7CO]^+$, 23), 1058 ($[M - 8CO]^+$, 13), 1030 ($[M - 9CO]^+$, 8), 1002 ($[M - 10CO]^+$, 10).

**3**. Anal. Found: C, 39.52; H, 2.14%. $C_{50}H_{35}Ir_3MoO_9P_2$. Calc.: C, 39.66; H, 2.33%. IR (c-$C_6H_{12}$): $\nu$(CO) 2062vs, 2029w, 2011s, 2004vs, 1989vs, 1961m, 1915w, 1895m, 1816m, 1775s, 1763s, 1753s $cm^{-1}$. $^1H$ NMR ($CDCl_3$): $\delta$ 7.60–7.24 (m, 30H, Ph), 4.92 (s, 5H, $C_5H_5$) ppm. $^{31}P$ NMR ($CDCl_3$, 230 K): 27.1 (s, 4P), 25.6 (s, 1P), −7.0 (s, 1P) ppm. MS: 1516 ($[M]^+$, 8), 1488 ($[M - CO]^+$, 10), 1460 ($[M - 2CO]^+$, 28), 1432 ($[M - 3CO]^+$, 66), 1404 ($[M - 4CO]^+$, 10), 1376 ($[M - 5CO]^+$, 100), 1348 ($[M - 6CO]^+$, 40), 1320 ($[M - 7CO]^+$, 46), 1271 ($[M - 6CO - Ph]^+$, 19), 1243 ($[M - 7CO - Ph]^+$, 21), 1166 ($[M - 7CO - 2Ph]^+$, 29), 1101 ($[M - 7CO - 2Ph - Cp]^+$, 17), 1086 ($[M - 6CO - PPh_3]^+$, 22), 1058 ($[M - 7CO - PPh_3]^+$, 66), 1030 ($[M - 8CO - PPh_3]^+$, 11), 1009 ($[M - 6CO - PPh_3 - Ph]^+$, 8), 1002 ($[M - 9CO - PPh_3]^+$, 12), 981 ($[M - 7CO - PPh_3 - Ph]^+$, 12), 953 ($[M - 8CO - PPh_3 - Ph]^+$, 44), 925 ($[M - 9CO - PPh_3 - Ph]^+$, 23).

### *3.8. Reaction of $CpMoIr_3(\mu\text{-}CO)_3(CO)_8$ with 1 equiv. of $PMe_3$*

An orange solution of $CpMoIr_3(\mu\text{-}CO)_3(CO)_8$ (27.2 mg, 0.0260 mmol) and $PMe_3$ (27 μl, 1 M solution in THF, 0.027 mmol) in THF (25 ml) was stirred at room temperature for 24 h. The dark orange solution obtained was evaporated to dryness on a rotary evaporator, then the residue dissolved in $CH_2Cl_2$ (ca. 3 ml) and applied to preparative chromatographic plates. Elution with dichloromethane–petroleum spirit (3/2) gave three bands. The contents of the first band, $R_f = 0.76$, were identified by solution IR as unreacted $CpMoIr_3(\mu\text{-}CO)_3(CO)_8$ (**1**) (4.2 mg, 0.0040 mmol (15%)). The second and major band, $R_f = 0.60$, was crystallized from $CHCl_3$–MeOH to afford orange crystals of $CpMoIr_3(\mu\text{-}CO)_3(CO)_7(PMe_3)$ (**4**) (12.7 mg, 0.0116 mmol (45%)). The third band, $R_f = 0.43$, was crystallized from $CHCl_3$–MeOH to afford orange crystals of $CpMoIr_3(\mu\text{-}CO)_3(CO)_6(PMe_3)_2$ (**5**) (10.6 mg, 0.0093 mmol (36%)).

### *3.9. Reaction of $CpMoIr_3(\mu\text{-}CO)_3(CO)_8$ with 2 equiv. of $PMe_3$*

Following the method in Section 3.8, $CpMoIr_3(\mu\text{-}CO)_3(CO)_8$ (25.6 mg, 0.0245 mmol) was reacted with $PMe_3$ (49 μl, 1 M solution in THF, 0.049 mmol) in THF (25 ml) at room temperature for 24 h. Purification by preparative chromatography with dichloromethane–petroleum spirit (3/2) eluent gave three bands. The first band, $R_f = 0.74$, was identified by solution IR as $CpMoIr_3(\mu\text{-}CO)_3(CO)_8$ (1.8 mg, 0.0017 mmol (7%)) (**1**). The second band, $R_f = 0.58$, was identified by IR and $^1H$ NMR as $CpMoIr_3(\mu\text{-}CO)_3(CO)_7(PMe_3)$ (**4**) (1.2 mg, 0.0011 mmol (5%)). The major band, $R_f = 0.45$, was identified by IR and $^1H$ NMR as $CpMoIr_3(\mu\text{-}CO)_3(CO)_6(PMe_3)_2$ (**5**) (13.0 mg, 0.0114 mmol (46%)).

### *3.10. Reaction of $CpMoIr_3(\mu\text{-}CO)_3(CO)_8$ with 3 equiv. of $PMe_3$*

Following the method in Section 3.8, $CpMoIr_3(\mu\text{-}CO)_3(CO)_8$ (28.0 mg, 0.0268 mmol) was reacted with $PMe_3$ (78 μl, 1 M solution in THF, 0.078 mmol) in THF (25 ml) at room temperature for 24 h. Purification by preparative chromatography with dichloromethane–petroleum spirit (3/2) eluent gave two bands. The first, $R_f = 0.47$, was identified by IR and $^1H$ NMR as $CpMoIr_3(\mu\text{-}CO)_3(CO)_6(PMe_3)_2$ (**5**) (4.0 mg, 0.0035 mmol (13%)). The second band, $R_f = 0.20$, was identified as $CpMoIr_3(\mu\text{-}CO)_3(CO)_5(PMe_3)_3$ (**6**) (9.3 mg, 0.0078 mmol (30%)).

### *3.11. Reaction of $CpMoIr_3(\mu\text{-}CO)_3(CO)_8$ with excess $PMe_3$*

Following the method in Section 3.8, $CpMoIr_3(\mu\text{-}CO)_3(CO)_8$ (35.2 mg, 0.0337 mmol) was reacted with $PMe_3$ (202 μl, 1 M solution in THF, 0.202 mmol) in THF (25 ml) at room temperature for 24 h. Purification by preparative chromatography with dichloromethane–petroleum spirit (3/2) eluent gave two bands. The first, $R_f = 0.51$, in trace amounts, was identified by IR as $CpMoIr_3(\mu\text{-}CO)_3(CO)_6(PMe_3)_2$ (**5**). The major band, $R_f = 0.24$, was identified by IR and $^1H$ NMR as $CpMoIr_3(\mu\text{-}CO)_3(CO)_5(PMe_3)_3$ (**6**) (13.6 mg, 0.0114 mmol (34%)).

### *3.12. Analytical data for **4**, **5** and **6***

**4**. Anal. Found: C, 20.42; H, 1.04%. $C_{18}H_{14}Ir_3MoO_{10}P$. Calc.: C, 19.77; H, 1.29%. IR (c-$C_6H_{12}$): $\nu$(CO) 2072s, 2063w, 2043vs, 2032m, 2024s, 2016s, 2013vs, 2006s, 1996vs, 1993s, 1985w, 1962w, 1927w, 1908w, 1842w, 1825m, 1807m, 1764m $cm^{-1}$. $^1H$ NMR ($CDCl_3$): $\delta$ 5.01 (s, 5H, $C_5H_5$), 1.90 (d, $J$(HP) = 11 Hz, 9H, Me) ppm. $^{31}P$ NMR ($CDCl_3$, 230 K): −26.2 (s, 1P) ppm. MS: 1096 ($[M]^+$, 29), 1068 ($[M - CO]^+$, 24), 1040 ($[M - 2CO]^+$, 52), 1012 ($[M - 3CO]^+$, 100), 984 ($[M - 4CO]^+$, 40), 956 ($[M - 5CO]^+$, 43), 928 ($[M - 6CO]^+$, 50), 913 ($[M - 6CO - Me]^+$, 12), 900 ($[M - 7CO]^+$, 43), 880 ($[M - 5CO - PMe_3]^+$, 16), 870 ($[M - 7CO - 2Me]^+$, 29), 852 ($[M - 6CO - PMe_3]^+$, 23), 842 ($[M - 8CO - 2Me]^+$, 17), 824 ($[M - 7CO - PMe_3]^+$, 21), 814 ($[M - 9CO - 2Me]^+$, 17), 796 ($[M - 8CO - PMe_3]^+$, 10), 786 ($[M - 10CO - 2Me]^+$, 7).

**5**. Anal. Found: C, 22.18; H, 1.91%.

$C_{20}H_{23}Ir_3MoO_9P_2$. Calc.: C, 21.04; H, 2.03%. IR (c-$C_6H_{12}$): $\nu$(CO) 2046m, 2006vs, 1996sh, 1192vs, 1985m, 1978m, 1968m, 1955m, 1891w, 1813w, 1768m, 1751m $cm^{-1}$. $^1H$ NMR ($CDCl_3$): $\delta$ 5.04 (s, 5H, $C_5H_5$), 1.94 (d, $J$(HP) = 10 Hz, 18H, Me) ppm. $^{31}P$ NMR ($CDCl_3$, 230 K): −21.8 (s, 3P), −23.8 (s, 1P), −41.8 (s, 1P) ppm. MS: 1116 ([M − CO]$^+$, 10), 1088 ([M − 2CO]$^+$, 28), 1060 ([M − 3CO]$^+$, 90), 1032 ([M − 4CO]$^+$, 50), 1004 ([M − 5CO]$^+$, 50), 974 ([M − 5CO − 2Me]$^+$, 100), 956 ([M − 4CO − $PMe_3$]$^+$, 27), 946 ([M − 6CO − Me]$^+$, 52), 928 ([M − 5CO − $PMe_3$]$^+$, 41), 913 ([M − 5CO − $PMe_3$ − Me]$^+$, 38), 898 ([M − 5CO − $PMe_3$ − 2Me]$^+$, 47), 885 ([M − 6CO − $PMe_3$ − Me]$^+$, 39), 870 ([M − 6CO − $PMe_3$ − 2Me]$^+$, 41), 857 ([M − 7CO − $PMe_3$ − Me]$^+$, 45), 842 ([M − 7CO − $PMe_3$ − 2Me]$^+$, 37), 827 ([M − 7CO − $PMe_3$ − 3Me]$^+$, 22).

**6**. IR (c-$C_6H_{12}$): $\nu$(CO) 2007s, 1967vs, 1960s, 1951 s, 1782s, 1756m, 1737s $cm^{-1}$. $^1H$ NMR ($CDCl_3$): $\delta$ 4.89 (s, 5H, $C_5H_5$), 1.79 (s (br), 27H, Me) ppm. $^{31}P$ NMR ($CDCl_3$, 230 K): −28.1 (s, P), −46.7 (s, 1P), −80.1 (s, 1P) ppm. MS: 1192 ([M]$^+$, 68), 1164 ([M − CO]$^+$, 100), 1136 ([M − 2CO]$^+$, 52), 1108 ([M − 3CO]$^+$, 77), 1080 ([M − 4CO]$^+$, 38), 1060 ([M − 2CO − $PMe_3$]$^+$, 52), 1052 ([M − 5CO]$^+$, 62), 1032 ([M − 3CO − $PMe_3$]$^+$, 53), 1022 ([M − 5CO − 2Me]$^+$, 48), 1004 ([M − 4CO − $PMe_3$]$^+$, 45), 989 ([M − $PMe_3$ − Me]$^+$, 59), 976 ([M − 5CO − $PMe_3$]$^+$, 55), 961 (M − 5CO − $PMe_3$ − Me]$^+$, 45), 946 ([M − 5CO − $PMe_3$ − 2Me]$^+$, 73), 933 ([M − 6CO − $PMe_3$ − Me]$^+$, 46), 918 ([M − 6CO − $PMe_3$ − 2Me]$^+$, 58), 905 ([M − 7CO − $PMe_3$ − Me]$^+$, 81), 890 ([M − 7CO − $PMe_3$ − 2Me]$^+$, 45), 857 ([M − 6CO − 2$PMe_3$ − Me]$^+$, 48).

### 3.13. X-ray structure determination

An orange-red block of $CpMoIr_3(\mu\text{-}CO)_3(CO)_7(PPh_3)$ (**2a**) suitable for diffraction analysis was grown by slow diffusion of methanol into a dichloromethane solution at 3 °C. A unique diffractometer data set was collected on a Rigaku AFC6R diffractometer at 298 K within the $2\theta_{max}$ limit 50.1° ($\omega$–$2\theta$ scan mode; monochromatic Mo K$\alpha$ radiation ($\lambda$ = 0.71069 Å) yielding 6258 independent reflections. 4359 of these with $I > 3\sigma(I)$ were considered 'observed' and used in the full-matrix least squares refinement after Lorentz-polarization, empirical absorption (transmission factors 0.34–1.00) and secondary extinction corrections. Anisotropic thermal parameters were refined for the non-hydrogen atoms; $(x, y, z, U_{iso})_H$ were included, constrained at estimated values. Conventional residuals $R = 0.034$ and $R_w = 0.031$ on $|F|$ at convergence were obtained, the weighting function $w = 4F_o^2/\sigma^2(F_o^2)$ where $\sigma^2(F_o^2) = [S^2(C + 4B) + (pF_o^2)^2]/Lp^2$ ($S$ is the scan rate, $C$ is the peak count, $B$ is the background count, $p = 0.01$ determined experimentally from standard reflections) being employed. Computation used the TEXSAN package [8]. Pertinent results are given in the figures and tables. Tables of hydrogen atom coordinates and thermal parameters and complete lists of bond lengths and angles for non-hydrogen atoms have been deposited at the Cambridge Crystallographic Data Centre.

### 3.14. Crystal data

$C_{33}H_{20}Ir_3MoO_{10}P$, $M = 1280.09$. Monoclinic, space group $P2_1/c$ (№ 14), $a = 9.804(3)$, $b = 15.071(4)$, $c = 23.407(9)$ Å, $\beta = 101.55(2)°$, $V = 3388(1)$ Å$^3$, $Z = 4$. $D_{calc} = 2.509$ g $cm^{-3}$; $F(000) = 2344$. $\mu_{Mo} = 121.62$ $cm^{-1}$; specimen: 0.44 × 0.40 × 0.20 $mm^3$; $T_{min,max} = 0.34, 1.00$.

## Acknowledgements

We thank the Australian Research Council for support of this work and Johnson–Matthey Technology Centre for a generous loan of iridium salts. MGH holds an ARC Australian Research Fellowship and NTL holds an RSC Honours Year Scholarship.

## References

[1] N.T. Lucas, M.G. Humphrey, D.C.R. Hockless, J. Organomet. Chem. 535 (1997) 177–183.
[2] J. Lee, M.G. Humphrey, D.C.R. Hockless, B.W. Skelton, A.H. White, Organometallics 12 (1993) 3468.
[3] S.M. Waterman, M.G. Humphrey, V.-A. Tolhurst, B.W. Skelton, A.H. White, D.C.R. Hockless, Organometallics 15 (1996) 934.
[4] S.M. Waterman, V.-A. Tolhurst, M.G. Humphrey, B.W. Skelton, A.H. White, J. Organomet. Chem. 515 (1996) 89.
[5] S.M. Waterman, M.G. Humphrey, D.C.R. Hockless, Organometallics 15 (1996) 1745.
[6] M. Bojczuk, B.T. Heaton, S. Johnson, C.A. Ghilardi, A. Orlandini, J. Organomet. Chem. 341 (1988) 473.
[7] M.R. Churchill, Y. Li, J.R. Shapley, D.S. Foose, W.S. Uchiyama, J. Organomet. Chem. 312 (1986) 121.
[8] TEXSAN, Single Crystal Structure Analysis Software, Version 1.6c, Molecular Structure Corporation, The Woodlands, TX, 1993.